

Thermoelectric porous MOF based hybrid materials

Cite as: APL Mater. **8**, 060902 (2020); <https://doi.org/10.1063/5.0004699>

Submitted: 17 February 2020 . Accepted: 22 May 2020 . Published Online: 11 June 2020

Engelbert Redel , and Helmut Baumgart 



View Online



Export Citation



CrossMark

ARTICLES YOU MAY BE INTERESTED IN

P-block metal-based (Sn, In, Bi, Pb) electrocatalysts for selective reduction of CO₂ to formate

APL Materials **8**, 060901 (2020); <https://doi.org/10.1063/5.0004194>

Rare-earth based half-Heusler topological quantum materials: A perspective

APL Materials **8**, 060903 (2020); <https://doi.org/10.1063/5.0006118>

Recent advances on visible-light-driven CO₂ reduction: Strategies for boosting solar energy transformation

APL Materials **8**, 060904 (2020); <https://doi.org/10.1063/5.0003215>

additive manufacturing epitaxial crystal growth cerium oxide polishing powder silver nanoparticles sputtering targets III-IV semiconductors CVD precursors europium phosphors

AMERICAN ELEMENTS

THE ADVANCED MATERIALS MANUFACTURER®

deposition slugs OLED Lighting spintronics solar energy osmium nanoribbons thin films chalcogenides AuNPs GDC Li-ion battery electrolytes 99.999% ruthenium spheres

endohedral fullerenes copper nanoparticles diamond micropowder CIGS MBE grade materials palladium catalysts flexible electronics beta-barium borate borosilicate glass dysprosium pellets YBCO pyrolytic graphite 3d graphene foam indium tin oxide mesoporous silica raman substrates sapphire windows tungsten carbide InGaAs barium fluoride carbon nanotubes lithium niobate scandium powder

gallium lump glassy carbon nanodispersions InAs wafers laser crystals ultra high purity materials MOFs rare earth metals photovoltaics refractory metals MOCVD organometallics quantum dot superconductors transparent ceramics ultra high purity silicon

American Elements opens up a world of possibilities so you can **Now Invent!**

Over 15,000 certified high purity laboratory chemicals, metals, & advanced materials and a state-of-the-art Research Center. Printable GHS-compliant Safety Data Sheets. Thousands of new products. And much more. All on a secure multi-language "Mobile Responsive" platform.

perovskite crystals yttrium iron garnet alternative energy h-BN gold nanocubes graphene oxide macromolecules photonics rhodium sponge fiber optics beamsplitters infrared dyes zeolites fused quartz metallocenes platinum ink buckyballs Ti-6Al-4V

Now Invent.™
The Next Generation of Material Science Catalogs

www.americanelements.com

Thermoelectric porous MOF based hybrid materials

Cite as: APL Mater. 8, 060902 (2020); doi: 10.1063/5.0004699

Submitted: 17 February 2020 • Accepted: 22 May 2020 •

Published Online: 11 June 2020



View Online



Export Citation



CrossMark

Engelbert Redel^{1,a)}  and Helmut Baumgart² 

AFFILIATIONS

¹Institute of Functional Interfaces (IFG), Karlsruhe Institute of Technology (KIT), Karlsruhe, Germany

²Department of Electrical and Computer Engineering, Old Dominion University, Norfolk, Virginia 23529, USA

^{a)}Author to whom correspondence should be addressed: Engelbert.Redel@kit.edu

ABSTRACT

Porous hybrid materials and MOF (Metal–Organic–Framework) films represent modern designer materials that exhibit many requirements of a near ideal and tunable future thermoelectric (TE) material. In contrast to traditional semiconducting bulk TE materials, porous hybrid MOF templates can be used to overcome some of the constraints of physics in bulk TE materials. These porous hybrid systems are amenable for simulation and modeling to design novel optimized electron–crystal phonon–glass materials with potentially very high ZT (figure of merit) numbers. Porous MOF and hybrid materials possess an ultra-low thermal conductivity, which can be further modulated by phonon engineering within their complex porous and hierarchical architecture to advance the TE figure of merit (ZT). This Perspective review discusses recent results of MOF TE materials and provides a future outlook and the vision to the search for the next generation TE porous hybrid and MOF materials, which could be part of the green renewable energy revolution with novel materials of sustainably high ZT values.

© 2020 Author(s). All article content, except where otherwise noted, is licensed under a Creative Commons Attribution (CC BY) license (<http://creativecommons.org/licenses/by/4.0/>). <https://doi.org/10.1063/5.0004699>

INTRODUCTION

Aside from the over-reliance on fossil fuels, one of the many challenges of the energy use in the modern post-industrial society is the huge untapped amount of waste heat generated, which cannot be economically harnessed and utilized with today's thermoelectric (TE) materials.

Basically, all industrial machinery, the huge number of combustion engines and batteries in automobiles, thermal power plants, nuclear power plants, waste incinerators, and most technological equipment produce heat even including our human bodies, which when being left untapped is forever lost, counting almost $\approx 70\%$ of the total energy used today.¹

Therefore, to move forward and to tap this mostly unused resource, i.e., waste heat recovery, much more efficient thermoelectric materials with a ZT larger than 3 are required, which can efficiently convert waste heat into green and renewable electricity.

Tackling this challenging problem could provide a path to green energy revolution and could provide advanced materials and devices, which can change our energy system and make significant

contributions to lessen the reliance on fossil fuels. If we are taking a bold hypothetical future outlook, our world would appear, for example, as follows:

- Novel thermoelectric materials could provide efficient solid-state cooling to replace freon based conventional refrigerators when inexpensive thermoelectric materials reach a $ZT \approx 3$.
- Mass production of novel thermoelectric generators (TEGs) and hybrid thermoelectrics with ZT over ≈ 3 would definitely transform our energy system and make an impact on the whole world.
- Thermoelectrics with a ZT of ≈ 5 could be synthesized with novel material systems, which might have twice the efficiency of combustion engines and refrigerators, and would be lighter, smaller, and more reliable.

The history of thermoelectrics (TEs) began in 1822, when German physicist Thomas Johann Seebeck discovered the effect, when he experimentally found that a compass needle was deflected by a closed loop connecting two dissimilar metal junctions, which were

exposed to a temperature difference.² This was interpreted as a potential difference arising from the temperature gradient between the junctions causing an electric current, which, in turn, induced a magnetic field to deflect the compass needle. In case one junction is open, while the temperature differential is maintained, no current is flowing, but the Seebeck voltage can be measured across the open circuit. This generated voltage V is a function of the temperature gradient ΔT and is related by a proportionality constant, known as the Seebeck coefficient S or thermopower, according to the relation $V = S \Delta T$. At the most basic level, the Seebeck effect can be described as the conversion of a temperature difference into an electric current. In his honor, the direct conversion from heat gradients to electricity at the junction of two conductors was later named the Seebeck effect.³ Conversely, by passing an electric current through such a circuit with two junctions, heat is generated at one junction, while heat is removed at the other junction. Later on, this reverse effect was discovered in 1834 by French physicist Jean Peltier and was named the Peltier effect.⁴ Peltier heat at a junction is absorbed or liberated following the relationship $Q_{\text{Peltier}} = \Pi I$, where Π is the Peltier coefficient and I denotes the current. It is noteworthy that Peltier heating or cooling is reversible between heat and electricity. In 1851, the Thomson effect⁵ was discovered, which describes the phenomenon that heat power (Q_{Thomson}) is absorbed or evolved along the length of a material rod whose ends are at different temperatures. The Thomson heat Q_{Thomson} is proportional to both the electric current I and the temperature gradient ΔT according to the relation $Q_{\text{Thomson}} = -\tau I \Delta T$, where the proportionality factor τ is known as the Thomson coefficient. Thomson heat is unique because it is reversible between heat and electricity, whereas resistive Joule heating in a conducting wire or rod is instead irreversible. While these three thermoelectric effects are interrelated, the Seebeck effect governs the generation of electricity from waste heat with thermoelectric generators and defines the sum of all physical processes, which we know as thermoelectrics today.⁶

Although thermoelectric semiconducting materials were known for many decades, it took almost a century from the discovery of the effect to active research in the field; see Fig. 1(a).⁷ Intensive studies

have been started in the 1950s, when scientists were convinced that thermoelectrics would soon replace conventional refrigerators and heat engines.⁸ The further development of thermoelectric devices was soon overshadowed by the massive progress and success in the photovoltaics and battery sector.⁹ Despite its advantages, thermoelectrics was relegated to niche markets such as power generation for space travel or Peltier cooling in optoelectronics and small refrigerators or cooled driver seats in high end luxury automobiles.⁹ Currently all commercially available thermoelectric generators are handicapped by their very low conversion efficiencies, which are well below the fundamental thermodynamic (Carnot) limit due to the limited Figure of Merit (ZT)¹⁰ of the present inorganic thermoelectric materials, as illustrated in the overview of Fig. 1(a) below.

This figure of merit (ZT) was first formulated in 1909 by German scientist Altenkirch¹² as $Z = S^2\sigma/(\kappa_e + \kappa_L)$, where S is the Seebeck coefficient, σ is the electrical conductivity, T is the temperature in kelvin, κ_e is the thermal conductivity due to electrons, and κ_L is the lattice thermal conductivity due to phonons.¹ Much later, in the 1950s, this metric was popularized by Ioffe¹³ *et al.* as a dimensionless figure of merit by multiplying Z with T to arrive at ZT . After the early burst of research initiatives of the 1950s, progress slowed down markedly for many decades [see Fig. 1(a)] until the early 1990s, when novel approaches and discoveries were pursued such as quantum confined structures, e.g., 2D thermoelectric nanomaterials: quantum wells and superlattices.¹⁴ At the beginning of the 20th century, thermoelectric materials were extensively studied for applications in civilian and military use. From the 1990s, nanotechnology promised a significant increase in the thermoelectric figure of merit $ZT = S^2\sigma T/(\kappa_e + \kappa_L)$ by new approaches for the separation of the electric and thermal properties of a material.¹⁵ However, ZT values for inorganic thermoelectric materials have been stuck for decades at an efficiency level of $ZT \approx 1-1.5$; see Fig. 1(a). In retrospect, these ZT values will not significantly increase in conventional inorganic thermoelectric materials in the foreseeable time because these material parameters are subject to the following laws of physics: the *Wiedemann–Franz law* and the *Mott relation*; see also the section titled “Moving

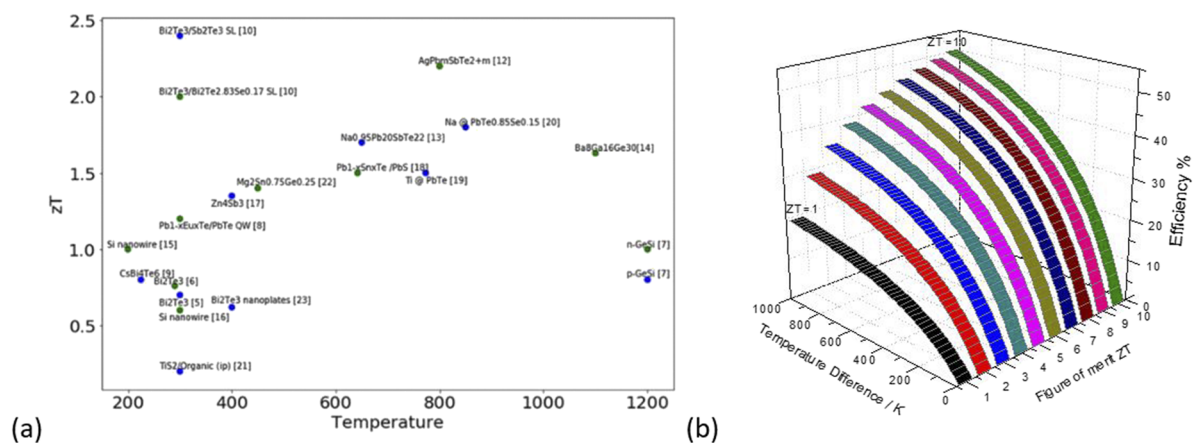


FIG. 1. (a) Major milestones of inorganic thermoelectric compounds achieved for ZT with permission from Ref. 11 and (Ref. 2–23 therein). (b) 3D graph of ZT plotting efficiency as a function of ZT and the temperature difference.¹¹

forward, unconventional thinking with unconventional materials is called for.” Basically, progress has been held back because of the fact that in conventional bulk thermoelectric materials, the quantities S , σ , and κ are interrelated in such a way as to make independent control of these variables to increase ZT almost impossible because an increase in S typically results in a decrease in σ and a decrease in σ produces a decrease in the electronic contribution to κ , according to the *Wiedemann–Franz law*. The advent of nanotechnology with a combination of small size and higher efficiency enabled thermoelectric applications that were unthinkable 20 years ago. Today, thermoelectric generators (TEGs) can be just a couple of millimeters in size and less than a millimeter thick, yet they contain hundreds of thermocouples.

By improving the ZT value with novel and non-traditional materials possessing very high theoretical ZT values, significant amounts of thermoelectric electricity can be generated from temperature differences of merely a few degrees; see Fig. 1(b). Modeling results indicate that, with novel optimized materials and new fabrication approaches, the power generation of thermoelectric devices with power conversion efficiency exceeding 20% is feasible, which significantly exceeds the state of the art, which is currently way below 12% for commercially available modules. Since ZT is inversely proportional to the thermal conductivity κ , it is imperative to decrease significantly the thermal conductivity and to decouple that change in thermal conductivity κ from the Seebeck coefficient S and the electrical conductivity σ . This objective can be achieved by localizing or trapping phonons within the materials. Novel materials with a very low thermal conductivity close to zero will attain unexpectedly high ZT values. The higher the ZT values, the lower the required temperature gradient window. Traditional semiconductor (SC) materials with lower ZT values are requiring much larger temperature windows to generate significant amounts of electricity. For this reason, the world requires novel nontraditional ZT materials and nothing less than the vision of revolutionary ultrahigh efficiency thermoelectric materials synthesized with completely new fabrication principles.

Today, researchers are investigating flexible substrates, thermoelectric fabrics, and low-cost materials. Progress in non-traditional thermoelectric materials, such as MOF (Metal–Organic–Framework) films (SURMOFs) and hybrid materials, could soon lead to TEGs and cooling modules with higher efficiency suitable for commercial applications.¹⁶ Soon we could have thermoelectric foils or fibers directly woven into our clothing, which can utilize heat directly, i.e., conversion of our body heat to power, for medical equipment such as pacemakers or electroosmotic pumps to deliver insulin and other drugs.¹⁷ Such embedded thermoelectric generators will be able to cover large areas of our body or other arbitrary surfaces without detracting from the main function of fabrics—dressing people—and hardly be noticeable. The power generated in that fashion could power sensors, actuators, smart watches, medical equipment, or smartphones directly embedded in the garment without the need of physical recharging.¹⁷

Moving forward, unconventional thinking with unconventional materials is called for

From the perspective of next generation, novel advanced thermoelectric materials improving the figure of merit (ZT) have gained

a lot of attention for the design of novel future TE material architectures and compositions to replace traditional semiconductors.

Thermoelectric properties and relationships are subject to a few laws of physics, which are indicated below; see Fig. 2. For example, the Mott relation establishes that the Seebeck coefficient S is indirectly proportional with the charge carrier density n . Therefore, very high Seebeck values are predicted for materials with an extremely small charge carrier density n , such as in the case of quasi-insulators. Merely increasing the electrical conductivity σ of a conventional thermoelectric material will not improve the ZT value because the Seebeck coefficient will drop due to its inverse proportionality with increased electrical conductivity according to the Mott relation. By increasing the electrical conductivity in traditional semiconductor (SC) thermoelectric materials, the electronic component of the thermal conductivity will also proportionally increase according to the Wiedemann–Franz law. The *Wiedemann–Franz law* describes the relationship between electrical conductivity σ and the electronic thermal conductivity κ_e by the Lorentz number L_0 as follows: $\kappa_e = L_0\sigma T$, e.g., in metals.¹⁸

The more electrically conductive the material is, the higher the charge carrier density n is, and the higher the resulting electronic component of the thermal conductivity is. This trend is counter-productive to the improvement of ZT . These two laws of physics interrelate all relevant thermoelectric parameters in such a way as to frustrate any significant improvement. As a consequence, the figure of merit (ZT) (see Fig. 1) has remained at a pretty constant level slightly above 1, which cannot be easily overcome by traditional bulk thermoelectric materials. The challenge is to optimize the “power factor (PF),” the product of the Seebeck coefficient squared, and electrical conductivity ($=S^2\sigma$) and to find the best trade-off for the composition of the ideal future MOF based hybrid thermoelectric material. These trends have been established for the past decades in the field without any real improvement. Therefore, conventional bulk thermoelectric materials are simply “constrained” by their physical laws, which cannot be easily overcome with bulk materials, as indicated in Fig. 2. However, these issues and limitations by the above quoted laws of physics are moot for materials with reduced dimensionality, such as quantum wells (QWs) (2D), quantum wires (1D), and quantum dots (QDs) (0D), where the introduction of a new variable (length scale) permits decoupling of the aforementioned parameters and allows them to be optimized simultaneously.

The phonon glass electron crystal (PGEC) concept is used in modeling and is defined as a hypothetical material that possesses the ideal low thermal conductivity of glass and optimum high electrical conductivity of semiconducting crystals.²⁰ The ideal PGEC concept has served as a roadmap by pointing out that the general strategy of increasing the electrical conductivity and simultaneously decreasing the thermal conductivity of thermoelectric materials will lead to the desired improvement in ZT values. Implementing this strategy accounts for the recent successes in improving inorganic thermoelectric materials. While the electrical conductivity of semiconducting crystalline thermoelectric materials can be improved in a straightforward manner by highly doping the materials to enhance the charge carrier density, this approach cannot easily be implemented into MOFs. Improving the electrical conductivity imposes a special challenge to MOFs and requires novel strategies. However, reducing the thermal conductivity by phonon scattering with porous

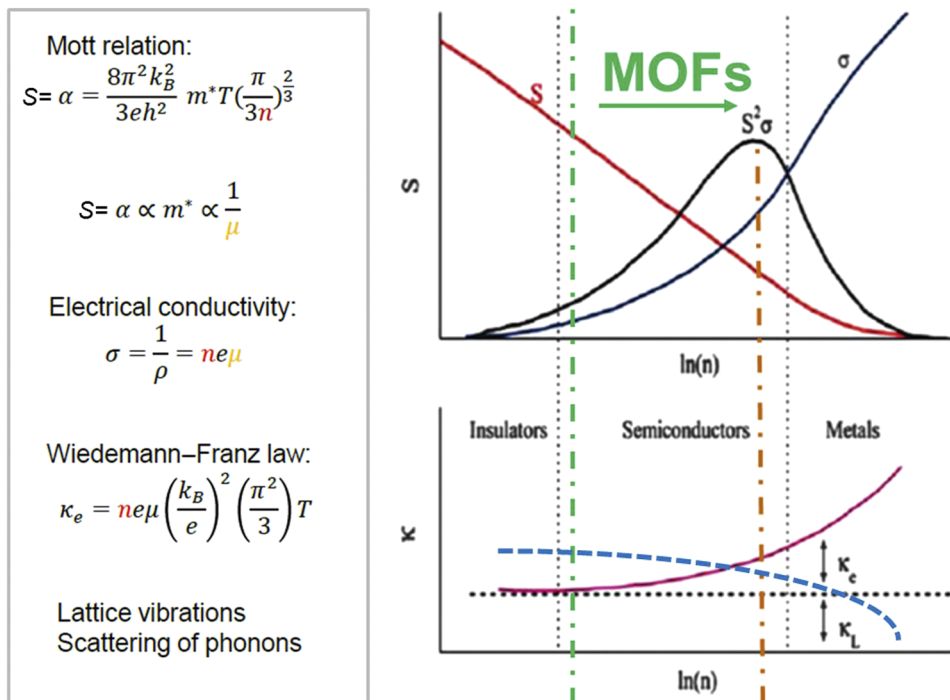


FIG. 2. On the left, the basic laws of physics governing thermoelectric relationships are shown. On the right, schematic plots of the Seebeck coefficient S and the thermal conductivity κ as a function of the natural logarithm of charge carrier density n are shown, adapted from Ref. 19.

templates works well in both inorganic thermoelectric materials and porous MOFs. Modeling of the phonon glass electron crystal (PGEC) concept revealed that successful reduction of thermal conductivity can be realized in a cage-like “open structured” compound as a host crystal, where heavy mass atoms are trapped inside, acting as scattering centers of phonons, to reduce thermal conductivity. Experimentally, skutterudites and intermetallic clathrates come very close to the ideal phonon glass electron crystals. Reduction of thermal conductivity is a universal key strategy for the enhancement of ZT . Therefore, the two-pronged strategy of increasing electrical conductivity, while decreasing thermal conductivity, is valid for inorganic and hybrid MOF materials but requires a different implementation for optimizing the electrical conductivity due to the chemo-physical properties of MOFs and coordination polymers (CPs).

In the future, novel designs of porous hybrid materials and metal–organic materials have the potential to overcome some of the constraints of physical laws that have handicapped conventional semiconducting bulk thermoelectric materials. As these materials can be simulated and modeled by their composition, pore size, and physical properties, a new thermoelectric material design with unexpectedly high ZT values might be feasible in the near future. This could potentially lead to materials revolutionizing our energy systems.

The magic impact of working with “nanoscaled” pores in porous templates

Pores/holes in porous templates constitute simply a “major impediment for phonon transport,” especially if the pore dimension is

of the order of magnitude of the mean-free path of phonons for that material. Every time a phonon encounters a pore/hole, the phonon will be scattered and loses energy. Therefore, the simulation-based prediction of hierarchical and porous architectures plays a major role in the design of novel thermoelectric materials. The smaller the pores are, the more complex the porous structure or architecture is designed, and the more the phonon transport will be impeded across the structure/architecture lattice, and therefore, the Thermal Lattice Conductivity (TLC) will be highly reduced. To maximize the impediment effect against phonon transport, the basic guiding principle stipulates that the pore dimensions should approximate the mean-free path of the phonons in the respective material. Different models have been reported²¹ in a porous “gray” material, as schematically depicted in Figs. 3(a) and 3(b). To illustrate the potential of the novel phonon engineering concept in nanostructured porous materials, the plots of Fig. 3(c) provide experimental examples of how the Seebeck coefficient S of the thermoelectric nanolaminate material system PbTe/PbSe has been modulated by phonon engineering utilizing porous templates and porous membranes. Because of the novelty aspect, there are hardly any literature reports on phonon engineering in porous MOF materials but have been reported for other inorganic thermoelectric systems. The potential benefits of phonon engineering in porous membranes have been theoretically modeled at MIT by the group of Romano.^{22,23} These theoretical simulations have recently been verified experimentally with inorganic thermoelectric materials.^{11,24–26} The plots in Fig. 3(c) benchmark the Seebeck coefficient of the thermoelectric material system PbTe/PbSe for the case of planar non-porous PbTe/PbSe films vs the case of porous templates with successive higher pore density.¹¹ For PbTe/PbSe thermoelectric films on planar non-structured

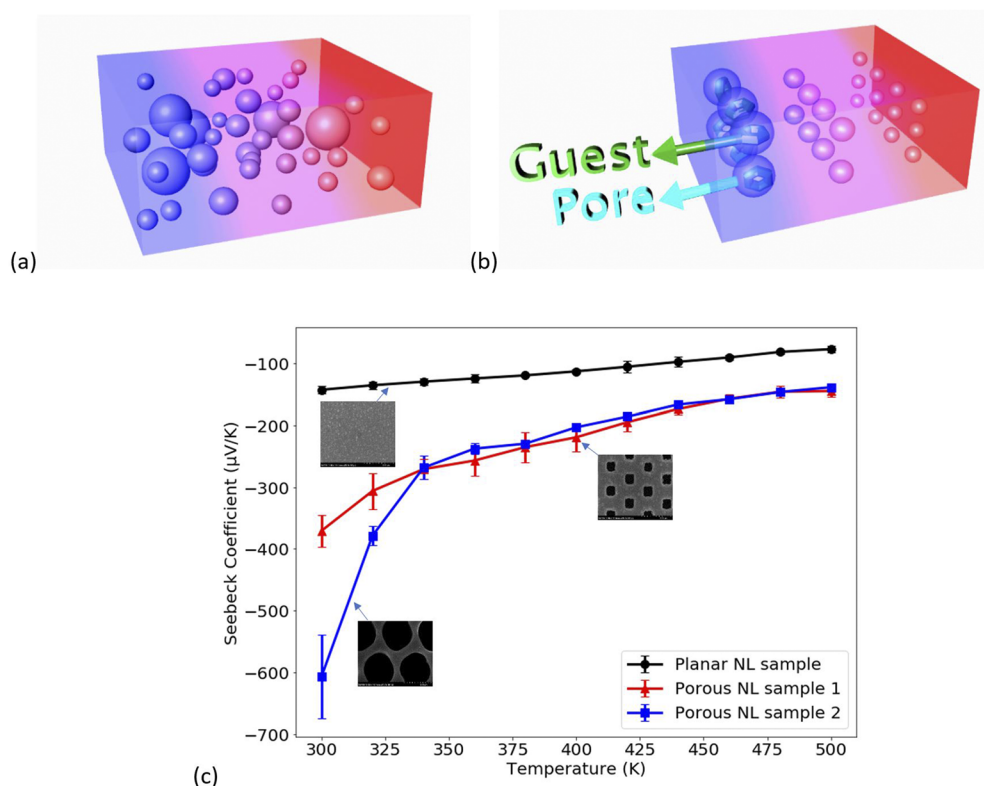


FIG. 3. (a) Schematic drawing of randomly oriented pores in a thermoelectric material. (b) Example of thermoelectric materials displaying different pore sizes, where the pores with the largest pore diameter have been infiltrated by super-positioned guest molecules. (c) Plots of the Seebeck coefficient of thermoelectric PbTe/PbSe films on the planar Si substrate benchmarked against PbTe/PbSe films on microporous Si substrates as a function of pore density and temperature. The nanostructured PbTe/PbSe films on the porous template with the highest pore density achieved a significant fourfold improvement for the Seebeck value,¹¹ which illustrates the benefits of phonon engineering in porous material systems.

Si substrates, the maximum Seebeck value measured was $-143.02 \pm 5.5 \mu\text{V/K}$ at 300 K, while the thermoelectric films on the porous Si substrate achieved an improved Seebeck value of $-370.5 \pm 37.7 \mu\text{V/K}$ for an intermediate pore density. For the higher pore density, the Seebeck value increased further to $-574.2 \pm 20.8 \mu\text{V/K}$ at 300 K, which amounts to a fourfold improvement for the Seebeck coefficient compared to the planar non-structured Si substrate. This example demonstrates the advantages of phonon engineering for the thermoelectric material system PbTe/PbSe in porous Si templates achieving significant improvements in the Seebeck coefficient as a function of pore density.¹¹

Some authors in the literature claimed that a 3D cubic lattice with identical holes is not possible.²⁰ However, 3D porous lattices are feasible in MOFs and porous hybrid materials, which can be loaded even with guest molecules, thereby further reducing the thermal conductivity. Loading of pores by guest molecules will induce additional phonon scattering, caused by a superposition of the guests. Recently, this effect has been demonstrated experimentally. Investigating these novel phenomena are part of the ongoing work in progress in our laboratories. It is feasible to synthesize highly 3D porous and hierarchical structures, which are designed to trap and to localize phonons within such structures or to severely impede

phonon transport, thereby creating a new generation of thermoelectric materials with ultra-low thermal conductivities or a heat insulator with extremely low thermal conductivity. The optimum thermoelectric material is a material possessing almost no thermal conductivity.

MATERIAL CHALLENGES

Porous hybrid materials and porous MOFs (Metal–Organic–Frameworks) and coordination polymers exhibit some promising material features that could predestine MOF and CNC (Coordination Network Compounds) films to be part of the next generation of future thermoelectric materials. From the definition of the IUPAC,²⁷ coordination polymers can be described as repeating coordination units with a 1D,²⁸ 2D,²⁹ or 3D³⁰ molecular structure. In contrast, MOFs describe coordination networks with organic ligands, which contain potential voids.³¹ In addition, the term MOF should also be exclusively used for carboxylate³² coordination networks. Of course, there are material challenges; however, the development pace and progress are fast and initial material issues appear manageable. High on the list of inherent advantages is the very

high Seebeck coefficient³³ and the possibility of designing optimized highly porous and complex hierarchical architectures.³⁴ Drawbacks are still today the low electrical conductivity in many MOF systems.³⁵ However, just recently, a major scientific breakthrough in advanced MOFs/porous hybrid materials has been reported with metallic conductivity behavior at room temperature.³⁶ Furthermore, intrinsic and extrinsic defects control many properties in these materials ranging from nucleation, growth, and hetero-integration to electronic and thermal transport. Defects in porous MOFs and hybrid materials come in all shapes and sizes, from point defects such as vacancies and impurities and two-dimensional defects such as grain boundaries. Therefore, all porous MOFs and hybrid materials contain structural defects that impact the physicochemical properties of the porous MOF layers.³⁷

OPPORTUNITIES—A BRIEF OVERVIEW

Hybrid and MOF thin film architectures have been created by the combination of different coatings and/or growth techniques, e.g., through spin-coating, anodic oxidation/electrochemical methods, liquid phase epitaxial (LPE) spray-coating, painting, dip-coating from suspensions, thin films sputtering, CVD, and liquid phase epitaxy (LPE). Regardless of the synthesis technique, most of them are based on a Layer by Layer (LbL) process, e.g., dip-coating, spin-coating, or spraying. In the past, some materials have been studied

only in their powder form, e.g., as pressed pellets. In the following, we provide a short review of recent results of porous hybrid and MOF systems, which have been published in the field since last year.

HKUST-1@TCNQ loaded with TCNQ

HKUST-1 MOF films (the acronym stands for Hong Kong University of Science and Technology) are constructed from Cu^{2+} dimers and benzene-tricarboxylate (BTC) units, which form a crystalline, 3D porous structure with a pore diameter of 1.2 nm, where the available pores allow the loading or storage of guest molecules, for example, TCNQ, inside the MOF structure [see Figs. 4(a) and 4(b)].

It is rather obvious that the electrical properties of porous MOFs/SURMOFs change when guest molecules are loaded into the pores of the framework. The first studies of this type were reported by Dragässer *et al.*, for the case of loading ferrocene inside monolithic HKUST-1 SURMOF thin films.³⁸ Later, Talin *et al.* found that after loading TCNQ (tetracyanoquinodimethane) molecules into the framework of HKUST-1, the electrical conductivity increased over six orders of magnitude with values up to 7 S m^{-1} in air.³⁹ First models have suggested that the conductivity arises from redox-active TCNQ guest molecules linking the copper paddle wheels within the open pores of HKUST-1.⁴⁰ Charge transport between the TCNQ guests has been recently described and theoretically

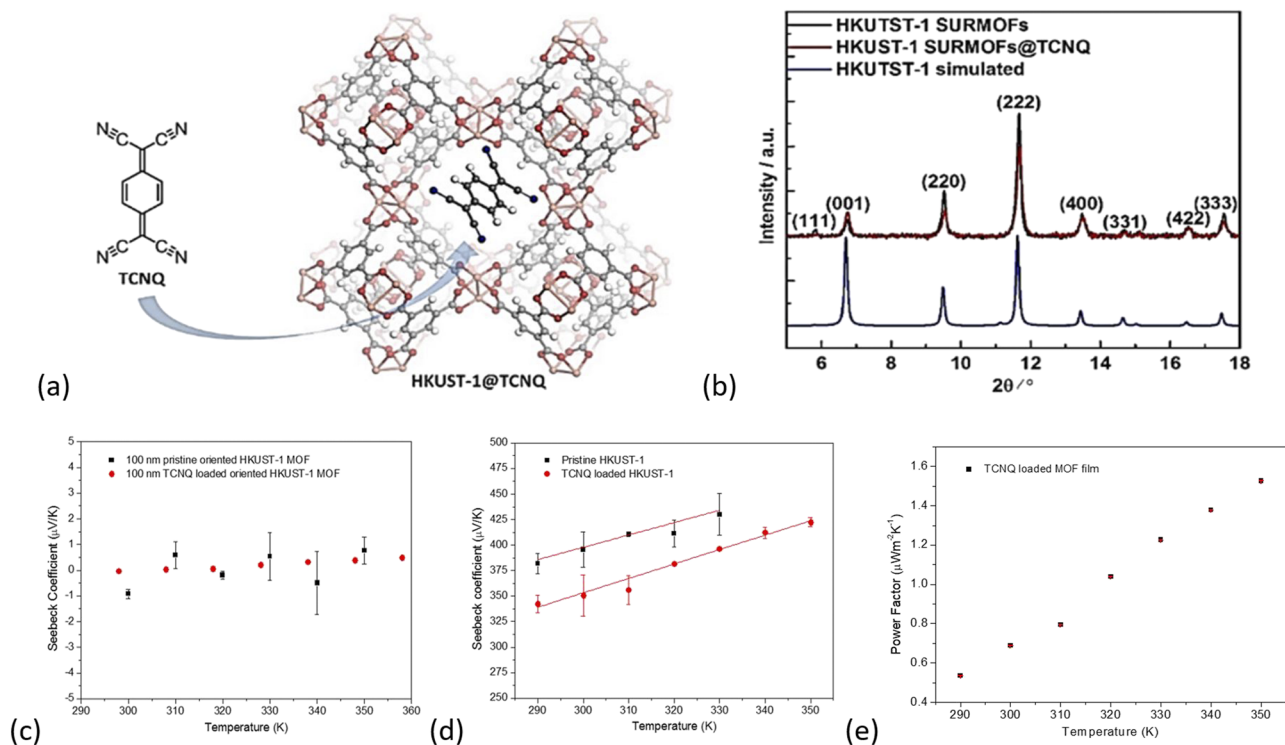


FIG. 4. (a) Schematic drawing of TCNQ infiltrated HKUST-1. (b) XRD of pristine, TCNQ infiltrated, and simulated HKUST-1 thin films. Seebeck coefficient measurements on (c) highly oriented HKUST-1 thin films,⁴³ (d) polycrystalline HKUST-1 thin films,⁴² and (e) power factor of TCNQ loaded HKUST-1 SURMOF.⁴⁴

investigated by a second-order process.⁴¹ In our own experimental studies, it was also pointed out that inconsistencies exist between the electronic-conducting mechanism proposed by these authors and the experimentally established positive sign of the Seebeck coefficient, which is a clear indication of a *p*-type conducting mechanism.⁴² Furthermore, we discovered that charge transfer and conductivity are highly anisotropic in MOF thin films. In this endeavor, we were able to measure the Seebeck coefficient in polycrystalline samples but not in highly oriented HKUST-1 thin films; see also Fig. 4(c).⁴³

Here, we have investigated the electrical properties of pristine HKUST-1 and TCNQ loaded compact HKUST-1 SURMOF films with Seebeck coefficient measurements.⁴² The compact MOF thin films were grown on pretreated Si substrates and on nonconductive borosilicate substrates using liquid phase epitaxy (LPE) in conjunction with a spray process already reported in our previous studies.⁴² This process yields MOF film thicknesses in the range of ≈ 40 – 100 nm, depending on the number of spraying cycles used. SURMOF films were characterized using x-ray diffraction and IRRAS measurements.

MOG–Ni₃(HITP)₂

A significant increase in the *ZT* has been reported through layered Ni₃(2,3,6,7,10,11-hexaimino-triphenylene)₂ [Ni₃(HITP)₂].⁴⁵ These materials can be described as a layered 2D lattice composed of Ni²⁺ ions, which are connected to (HITP³⁻) ligands, forming a honeycomb-like structure; see Fig. 5(a).⁴⁵ The individual layers are stacked, forming a graphite-like material, which are also known as Molecular-Organic Graphene (MOG) with 1.5 nm-wide tubular pores running parallel to the *c*-direction.⁴⁵ Therefore, a high anisotropic electrical conductivity (σ) of ~ 50 S cm⁻¹ was reported at room temperature, one of the highest among polycrystalline MOF hybrid materials. This very high electrical conductivity also leads to a 17-fold improvement of the *ZT* in comparison with HKUST-1@TCNQ systems.⁴⁵

The material was characterized as pressed pellet powder with a negative room temperature Seebeck coefficient (*S*) of -11.9 V K⁻¹, describing an *n*-type conductivity semiconductor behavior.⁴⁵ Furthermore, the Seebeck coefficient *S* was shown to be quite constant over the measured temperature range, yielding a power factor (*PF*)

of 8.31×10^{-3} W m⁻¹ K⁻².⁴⁵ In addition, the thermal conductivity was also quite low with a value of around $k = 0.21$ W m⁻¹ K⁻¹, where k_L (lattice thermal conductivity) appears to be responsible for the main contribution; see Fig. 5(b). These measured values yielded an overall *ZT* of $\approx 1.25 \times 10^{-3}$ at room temperature; see Fig. 5(b).⁴⁵

Non-porous coordination polymers (CPs)

In contrast to porous MOFs, non-porous coordination polymers (CPs), such as poly[Cu_x(Cu-ethylenetetrathiolate)],⁴⁶ poly[Na_x(Ni-ett)], and poly(K_x[Ni-ett]),⁴⁷ should also be considered within the scope of this review; see Figs. 6(a)–6(c). These compounds consist of repeating units of metal–organic complexes.^{46,47} An entire series of this promising hybrid thermoelectric material has been successfully synthesized. In fact, the CP poly(K_x[Ni-ett]) is composed of Ni(II) ions, which are chemically bound to 1,1,2,2-ethylenetetrathiolate (ett), where potassium K⁺ is used to balance the charge.⁴⁷ However, for the present time, these coordination polymers hold the record for *n*-type coordination polymers (CPs) with the highest *ZT* of around 0.2 at room temperature; see Fig. 6(b).⁴⁷

For poly[Cu_x(Cu-ethylenetetrathiolate)], the experimentally determined Seebeck coefficient rises as a function of increasing temperature, the positive Seebeck coefficient sign implies *p*-type charge carriers in the polymer, and the thermal conductivity also rises with increasing temperature.⁴⁶ At 300 K, the following details have been reported: the power factor *PF* and *ZT* are 4.17 W m⁻¹ K⁻² and 2.66×10^{-3} W m⁻¹ K⁻², respectively, while the corresponding electrical conductivity, Seebeck coefficient, and thermal conductivity have been reported as $\sigma = 10.7$ S cm⁻¹, $S = 62.5$ V K⁻¹, and $\kappa = 0.47$ W m⁻¹ K⁻¹, respectively. At 400 K, the parameters reached the following values: (σ) 25.8 S cm⁻¹, (*S*) 77.5 V K⁻¹, and (κ) 0.57 W m⁻¹ K⁻¹, thereby resulting in a power factor *PF* of 15.5 W m⁻¹ K⁻² and a *ZT* of 0.011.⁴⁶ For the CP poly[Na_x(Ni-ett)], *ZT* is 0.042 at 300 K and the *ZT* can reach up to 0.10 at 440 K. For all the reported coordination polymers (CPs), it appears that the power factor *PF* and the *ZT* tend to increase as a function of increasing temperature. Furthermore, it has been reported that the *ZT* value of poly[Cu_x(Cu-ett)] varies between 0.002 and 0.014 in the temperature range from 230 K to 400 K.⁴⁶ This is the highest reported *ZT* value around

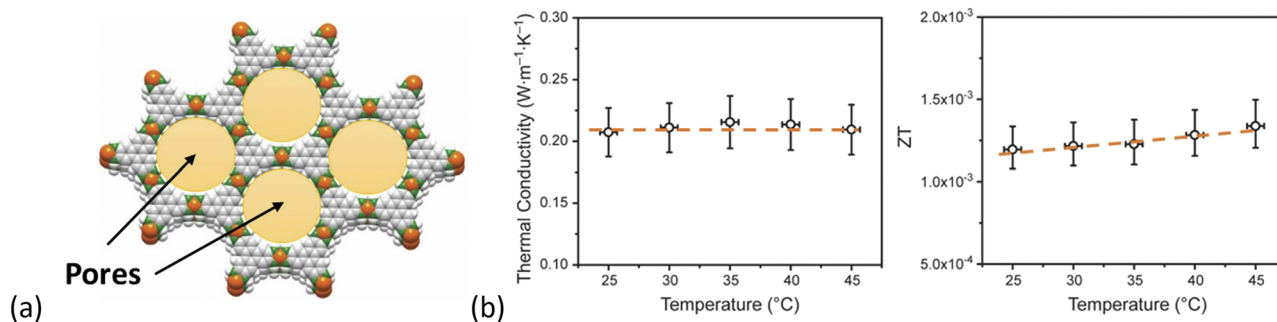


FIG. 5. (a) Schematic drawing of layered porous Ni₃(2,3,6,7,10,11-hexaimino-triphenylene)₂ [Ni₃(HITP)₂] MOG adapted from Ref. 45. (b) Thermal conductivity and *ZT* of Ni₃(HITP)₂ pressed powder pellets adapted with permission from Sun *et al.*, *Joule* 1, 168 (2017). Copyright 2017 Elsevier.⁴⁵

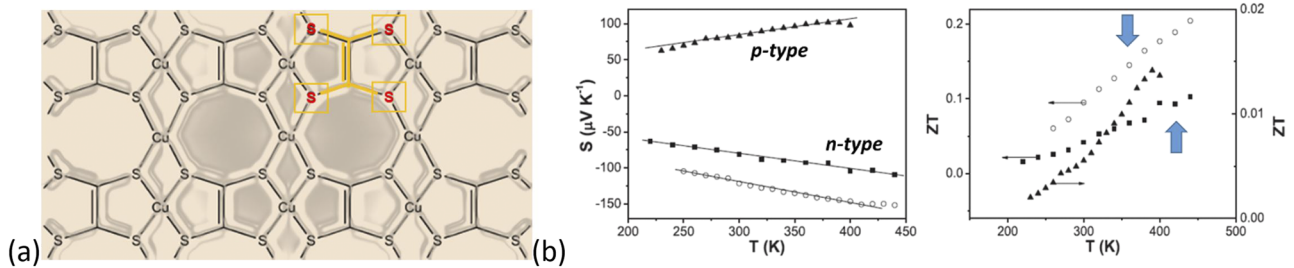


FIG. 6. (a) Schematic drawing of non-porous coordination polymers (CPs) poly[Cu_x(Cu-ethylenetetra-thiolate)] adapted from Ref. 46. (b) Seebeck coefficient and ZT of CPs poly[Na_x(Ni-ett)] and poly[K_x(Ni-ett)] adapted from Ref. 47.

0.014 (at 380 K), about one-order lower in comparison to that of nickel complexes poly[Na_x(Ni-ett)] and poly[K_x(Ni-ett)]; see also Fig. 6(b).⁴⁷

Polymer MOF based hybrid systems

Recently, nanocomposites prepared from MOF films and conducting polymers have been reported.⁴⁸ The polymers such as polypyrrole (PPy) and poly(3,4-ethylenedioxythiophene) (PEDOT) have been polymerized *in situ* in the voids of a UiO-66.⁴⁸ The polymerization has been characterized by various analytical techniques as well as HRTEM, revealing the successful incorporation of polymer fibers inside the voids of the framework. Furthermore, it was reported that in the polymerized UiO-66 composites, such as UiO-66-PPy and UiO-66-PEDOT, the thermal conductivity (κ) was significantly reduced.⁴⁸ The thermal conductivity for UiO-66 was determined as $\kappa \approx 0.8 \text{ W m}^{-1} \text{ K}^{-1}$, which is significantly lower in the case of UiO-66-PPy and UiO-66-PEDOT with values of $\kappa \approx 0.4 \text{ W m}^{-1} \text{ K}^{-1}$ and $\kappa \approx 0.3 \text{ W m}^{-1} \text{ K}^{-1}$.⁴⁸ However, the electrical conductivity was significantly increased by the incorporation of conductive polymers within the UiO-66 MOF.⁴⁸ The Seebeck

coefficient (S) and the Power Factor (PF) have not been reported in that study. Nanocomposites with an enhanced electrical conductivity with lowered thermal conductivity are promising for novel hybrid thermoelectric nanocomposite materials and thermoelectric generator (TEG) applications.⁴⁸

Screening platform: ZT chips form new thermoelectric hybrid materials

For screening purposes and in search for optimized future thermoelectric porous hybrid and MOF materials, a complete in-plane electric and thermoelectric characterization was successfully applied to spin-coated conductive PEDOT:PSS organic thin films.⁴⁹ To this end, a ZT lab-on-a-chip platform has been used; see Fig. 7(a) based on the Völklein geometry.⁵⁰ By utilizing such a ZT test chip, the electrical conductivity (σ), the resistivity (ρ), the Seebeck coefficient (S), the thermal conductivity (κ), the specific heat capacity (c_p), and, consequently, the power factor (PF) and ZT values have been determined simultaneously as a function of temperature with one single measurement run; see Fig. 7(b).⁴⁹ In addition, Hall measurements are possible with the same test chip design, which provides further

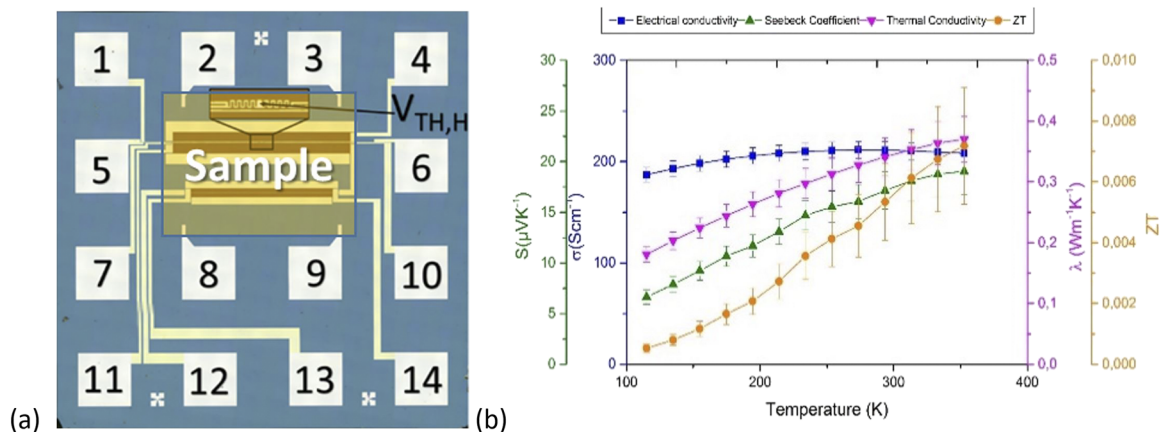


FIG. 7. (a) ZT test chip design for full electric and thermoelectric characterizations of conductive organic thin films adapted from Ref. 49. (b) Measured electrical and thermal conductivity and Seebeck coefficient and calculated ZT value of a 15 μm PEDOT:PSS thin film within the temperature range 110–420 K. The 15 μm thick poly(3,4-ethylenedioxythiophene) doped with a poly(styrene sulfonate) (PEDOT:PSS) film was prepared by drop casting.⁵¹

details on the mobility (μ) as well as the charge carrier concentration (n) of the examined thermoelectric materials.⁴⁹

Such ZT test chip tools will be deployed to efficiently test and prescreen which porous hybrid materials or MOF film composition possess the requisite properties for further material optimization toward real device applications.⁴⁹ The application potential includes custom designed thermoelectric thin film generators powered solely by the use of human body heat.

LOOKING FORWARD—FUTURE OUTLOOK ON NOVEL THERMOELECTRIC MATERIALS

Thermoelectric materials based on porous hybrid and MOFs constitute a very recent development, with many new and undiscovered phenomena for the research field. It is anticipated that especially the inherent porosity can be used advantageously in the design and simulation predictions of future thermoelectric materials. In principle, porous hybrid and MOF materials can comply with most of the requirements of an ideal and tunable future thermoelectric (TE) material. In contrast to traditional inorganic semiconductor (SC) materials, porous hybrid materials and MOFs have been demonstrated to be able to overcome the laws of physics governing bulk thermoelectric materials. These classes of novel materials offer new approaches to the design of complex and hierarchical porous structures, possessing ultra-low thermal conductivity, which are able to trap and localize phonons, thus resulting in a new generation of thermoelectric materials with a high ZT (figure of merit) number.

Therefore, as there are hardly any upper limits on the figure of merit (ZT), the quest for new and unexplored novel future thermoelectric materials is on.

This work demonstrates recent results of MOF TE materials and provides a vision and a future outlook for the search for tomorrow's novel thermoelectric MOF materials, which could be part of an anticipated green sustainable energy revolution with novel materials of high ZT values.

ACKNOWLEDGMENTS

E.R. acknowledges financial support by the Deutsche Forschungsgemeinschaft (DFG) within the Priority Program COORNET (Grant No. SPP 1928). H.B. acknowledges financial help from Old Dominion University. The authors would like to thank Donghui Chen for designing the images in Figs. 3(a) and 3(b).

REFERENCES

- D. M. Rowe, *Thermoelectrics Handbook: Macro to Nano* (Taylor & Francis Ltd., 2006), pp. 1–23.
- T. J. Seebeck, *Magnetic Polarization of Metals and Ores by Temperature Differences* (Abhandlungen der Königlichen Akademie der Wissenschaften zu Berlin, 1822), pp. 265–373.
- F. J. DiSalvo, *Science* **285**, 703 (1999).
- P. M. Peltier, *Ann. Chim. Phys.* **56**, 371 (1834).
- W. Thomson, “On a mechanical theory of thermo-electric currents,” *Proc. R. Soc. Edinburgh* **3**, 91–98 (1851).
- R. He, G. Schierning, and K. Nielsch, *Adv. Mater. Technol.* **3**, 1700256 (2018).
- C. J. Vineis, A. Shakouri, A. Majumdar, and M. G. Kanatzidis, *Adv. Mater.* **22**, 3970 (2010).

- D. Beretta, N. Neophytou, J. M. Hodges, M. G. Kanatzidis, D. Narducci, M. Martin-Gonzalez, M. Beekman, B. Balke, G. Cerretti, W. Tremel, A. Zevkink, A. I. Hofmann, C. Müller, B. Dörling, M. Campoy-Quiles, and M. Caironi, *Mater. Sci. Eng., R* **138**, 100501 (2019).
- L. F. Llin and D. J. Paul, in *ICT—Energy Concepts for Energy Efficiency and Sustainability* (InTechOpen, 2017), Chap. 9.
- Z.-G. Chen, G. Han, L. Yang, L. Cheng, and J. Zou, *Prog. Nat. Sci.: Mater. Int.* **12**, 535 (2012).
- X. Chen, P. Lin, K. Zhang, H. Baumgart, B. Geist, and V. Kochergin, *ECS J. Solid State Sci. Technol.* **5**(9), P503–P508 (2016).
- E. Altenkirch, “Über den nutzeffekt der thermosäule,” *Phys. Z.* **10**, 560 (1909).
- A. F. Ioffe, L. S. Stil’bans, E. K. Iordanishvili, T. S. Stavitskaya, and A. Gelbtuch, *Phys. Today* **12**(5), 42 (1959).
- J. Mao, Z. Liu, and Z. Ren, “Size effect in thermoelectric materials,” *npj Quantum Mater.* **1**, 16028 (2016).
- D. M. Rowe, *Thermoelectrics Handbook: Macro to Nano* (Taylor & Francis Ltd., 2006), pp. 54–112.
- H. Jin, J. Li, J. Iocozzia, X. Zeng, P. C. Wei, C. Yang, N. Li, Z. Liu, H. He, T. Zhu, J. Wang, Z. Lin, and S. Wang, *Angew. Chem., Int. Ed.* **58**, 15206 (2019).
- M. Culebras, C. M. Gómez, and A. Cantarero, *Materials* **7**, 6701 (2014).
- F. Völklein, H. Reith, T. W. Cornelius, M. Rauber, and R. Neumann, *Nanotechnology* **20**, 325706 (2009).
- C. Wood, “Materials for thermoelectric energy conversion,” *Rep. Prog. Phys.* **51**, 459 (1988).
- G. A. Slack, “Design concepts for improved thermoelectric materials,” in *MRS Online Proceedings Library Archive* (Cambridge University Press, Cambridge, UK, 1997), Vol. 478.
- R. H. Tarkhanyan and D. G. Niarchos, *APL Mater.* **2**, 076107 (2014).
- G. Romano, A. Di Carlo, and J. C. Grossman, *J. Comput. Electron.* **11**(1), 8 (2012).
- G. Romano and J. C. Grossman, *Appl. Phys. Lett.* **105**(3), 033116 (2014).
- M. Nomura, Y. Kage, J. Nakagawa, T. Hori, J. Maire, J. Shiomi, R. Anufriev, D. Moser, and O. Paul, *Phys. Rev. B* **91**(20), 205422 (2015).
- M. Nomura, Y. Kage, D. Müller, D. Moser, and O. Paul, *Appl. Phys. Lett.* **106**(22), 223106 (2015).
- X. Chen and H. Baumgart, *Materials* **13**, 1283 (2020).
- S. R. Batten, N. R. Champness, X.-M. Chen, J. Garcia-Martinez, S. Kitagawa, L. Öhrström, M. O’Keeffe, M. Paik Suh, and J. Reedijk, *Pure Appl. Chem.* **85**, 1715 (2013).
- F. Kübel and J. Strähle, *Z. Naturforsch., B* **37**, 272 (1982).
- D. Venkataraman, S. Lee, J. S. Moore, P. Zhang, K. A. Hirsch, G. B. Gardner, A. C. Covey, and C. L. Prentice, *Chem. Mater.* **8**, 2030 (1996).
- B. F. Abrahams, M. J. Hardie, B. F. Hoskins, R. Robson, and E. E. Sutherland, *J. Chem. Soc., Chem. Commun.* **1994**, 1049.
- H. Li, M. Eddaoudi, M. O’Keeffe, and O. M. Yaghi, *Nature* **402**, 276 (1999).
- S. S. Y. Chui, S. M. F. Lo, J. P. H. Charmant, A. G. Orpen, and I. D. Williams, *Science* **283**, 1148 (1999).
- K. J. Erickson, F. Léonard, V. Stavila, M. E. Foster, C. D. Spataru, R. E. Jones, B. M. Foley, P. E. Hopkins, M. D. Allendorf, and A. A. Talin, *Adv. Mater.* **27**, 3453 (2015).
- D. H. Chen, R. Haldar, B. L. Neumeier, Z. H. Fu, C. Feldmann, C. Wöll, and E. Redel, *Adv. Funct. Mat.* **29**, 1903086 (2019).
- A. A. Talin, R. E. Jones, and P. E. Hopkins, *MRS Bull.* **41**(11), 877–882 (2016).
- R. Dong, P. Han, H. Arora, M. Ballabio, M. Karakus, Z. Zhang, C. Shekhar, P. Adler, P. S. Petkov, A. Erbe, S. C. B. Mannsfeld, C. Felser, T. Heine, M. Bonn, X. Feng, and E. Cánovas, *Nat. Mater.* **17**, 1027 (2018).
- J. Liu and C. Wöll, *Chem. Soc. Rev.* **46**, 5730 (2017).
- A. Dragässer, O. Shekhah, O. Zybalyo, C. Shen, M. Buck, C. Wöll, and D. Schlettwein, *Chem. Commun.* **48**, 663 (2012).
- A. A. Talin, A. Centrene, A. C. Ford, M. E. Foster, V. Stavila, P. Haney, R. A. Kinney, V. Szalai, F. El Gabaly, H. P. Yoon *et al.*, *Science* **343**, 66 (2014).
- V. Stavila, A. A. Talin, and M. D. Allendorf, *Chem. Soc. Rev.* **43**, 5994 (2014).

- ⁴¹T. Neumann, J. Liu, T. Wächter, P. Friederich, F. Symalla, A. Welle, V. Mugnaini, V. Meded, M. Zharnikov, C. Wöll, and W. Wenzel, *ACS Nano* **10**, 7085 (2016).
- ⁴²X. Chen, Z. Wang, Z. M. Hassan, P. Lin, K. Zhang, H. Baumgart, and E. Redel, *ECS J. Solid State Sci. Technol.* **6**, P150 (2017).
- ⁴³X. Chen, Z. Wang, P. Lin, K. Zhang, H. Baumgart, E. Redel, and C. Wöll, *ECS Trans.* **75**, 119 (2016).
- ⁴⁴X. Chen and H. Baumgart, private communication (2017).
- ⁴⁵L. Sun, B. Liao, D. Sheberla, D. Kraemer, J. Zhou, E. A. Stach, D. Zakharov, V. Stavila, A. A. Talin, Y. Ge, M. D. Allendorf, G. Chen, F. Leonard, and M. Dincă, *Joule* **1**, 168 (2017).
- ⁴⁶P. Sheng, Y. Sun, F. Jiao, C. Liu, W. Xu, and D. Zhu, *Synth. Met.* **188**, 111 (2014).
- ⁴⁷Y. Sun, P. Sheng, C. Di, F. Jiao, D. Qiu, and D. Zhu, *Adv. Mater.* **24**, 932 (2012).
- ⁴⁸A. Jadhav, K. Gupta, P. Ninawe, and N. Ballav, *Angew. Chem., Int. Ed.* **59**, 2215 (2020).
- ⁴⁹V. Linseis, Z. M. Hassan, H. Reith, J. Garcia, K. Nielsch, H. Baumgart, E. Redel, and P. Woias, *Phys. Status Solidi A* **215**, 1700930 (2018).
- ⁵⁰V. Linseis, F. Völklein, H. Reith, P. Woias, and K. Nielsch, *J. Mater. Res.* **31**, 3196 (2016).
- ⁵¹V. Linseis, Linseis Company, private communication (2018).